Chinese Chemical Letters 35 (2024) 108408

Contents lists available at ScienceDirect

Chinese Chemical Letters

journal homepage: www.elsevier.com/locate/cclet

Evaluating the tumor stratification with a lysosomal pH sensitive-probe by fluorescence lifetime imaging

Jun Yan, Xing Liang, Qian Zhang, Luolin Wang, Weiying Lin*

Guangxi Key Laboratory of Electrochemical Energy Materials, Institute of Optical Materials and Chemical Biology, School of Chemistry and Chemical Engineering, Guangxi University, Nanning 530004, China

ARTICLE INFO

Article history:
Received 8 February 2023
Revised 26 March 2023
Accepted 29 March 2023
Available online 2 April 2023

Keywords:
FLIM
pH
Fluorescence imaging
Lysosome
Tumor imaging

ABSTRACT

Owing to the anaerobic metabolism in the tumor, abundant acidic metabolites are produced and accumulated in the cells. Therefore, the cells in different tumor layers are directly linked to the pH microenvironment. Nevertheless, due to the lack of robust tools, the high-efficient evaluation of the acidic micro-environment of tumor stratification faces the challenge of accurate diagnosis. We designed a new pH sensitive fluorescent lifetime probe target to lysosomes. As we expected, the fluorescence lifetime of **PLN** possesses a good linear fit to the pH value, which could detect the pH change at a single lysosome level in real time, and then evaluate the different acidity of tumor stratification. The probe **PLN** is successfully used to evaluate the tumor stratification by fluorescence lifetime imaging microscopy (FLIM) for the first time, which is of great significance in the preoperative diagnosis of clinical tumor treatment or evaluation of drug delivery effect.

Cancer has become the leading cause to the worldwide death, whose early detection, diagnosis and treatment are the key to its cure [1–3]. The carcinogenesis is a complex process characterized not only by abnormal proliferation, division and metastasis, but also by changes in the intracellular microenvironment such as pH, polarity, lack of oxygen and viscosity [1,4]. During the growth of tumor, due to the exuberant anaerobic metabolism in tumor tissue, a large number of acidic metabolites are produced, and the local vascular distribution in low density in tumor tissue makes the acidic metabolites hard to be discharged to the periphery of tumors and accumulated in the cells, which lead to the decrease of pH value [5]. Moreover, the intracellular pH is the core to the normal operation of various biological processes, and the stability of pH is crucial in these physiological and pathological processes, including cell proliferation, apoptosis, and endocytosis [6–8]. Therefore, monitoring pH changes is important in the fields of chemistry, biology, and medicine. Present in all eukaryotic cells, lysosomes are acidic organelles which play an important role in biological processes such as proteolysis, autophagy and apoptosis [9,10]. Abnormal lysosomal pH is strongly associated with cancer initiation and treatment [11–13]. Lysosomal pH in cancer cells (pH 3.8–4.7) [14,15] has been reported to be lower than that in normal cells (pH 4.5–6.0) [16–19]. It is particularly significant to develop a feasible and proven technique to detect lysosomal acidity.

Supported by fluorescence imaging techniques, many fluorescent probes have been developed to monitor lysosomal pH value [20–25]. As far, detection of lysosomal pH by fluorescence intensity variation has been reported in the literature [26]. However, the use of simple small molecules probes to detect the pH in a single lysosome level is still scarce. Due to the fluctuation of fluorescence intensity, the influence of excitation intensity, sample concentration and distribution will lead to biased results [27,28]. On the contrary, fluorescence lifetime imaging microscopy (FLIM) shows an evident superiority since it is immune to the variations in the excitation luminescence intensity and the concentration of the fluorophore [29–31]. Therefore, there is an urgent need to invent a FLIM-based fluorescent probe to evaluate the pH of lysosomes.

In this work, we reported a novel fluorescent lifetime probe **PLN** based on pyridine [32–35] to detect the variations pH of lysosomes. The fluorescence lifetime of **PLN** has a good linear fitting to the change of pH value. Throughout the experiment to adjust the acidity of cells in various external pH environments, it is verified that the probe can be used in FLIM imaging of living cells and detecting the pH microenvironment in cells. In addition, the probe **PLN** responded to the variations in lysosomal pH when the pH environment outside the cell changes. Furthermore, the probe **PLN** was used to determine the pH change of lysosomes under the stimulation of different drugs such as chloroquine [21,36,37],

* Corresponding author.
E-mail address: weiyinglin2013@163.com (W. Lin).

https://doi.org/10.1016/j.cclet.2023.108408
1001-8417/

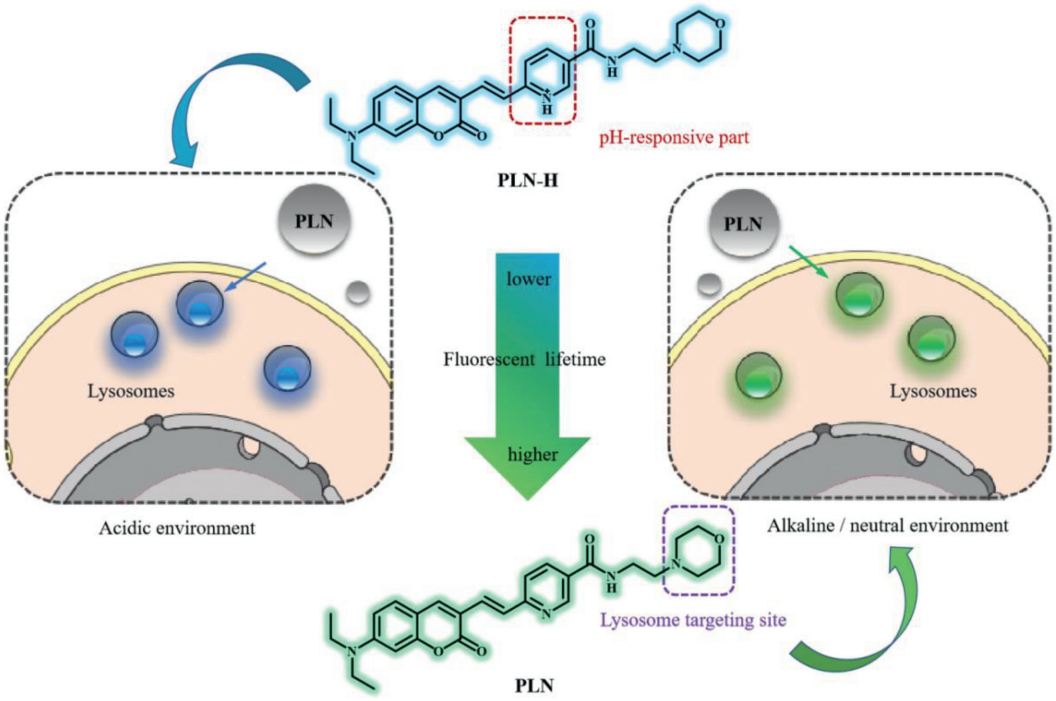

Scheme 1. The design concept of the probe **PLN**.

NH_4Cl [38], carbamazepine [1] and adenosine-triphosphate (ATP) [39]. Foremost, probe **PLN** has capacity in detecting the tumor stratification in accordance with the pH fluctuations at depths of various slices, offering a promising strategy to significantly realize the clinical treatment to tumors.

7-Diethylaminocoumarin fluorescence platform is characterized by its high fluorescence quantum yield and large absorption and emission spectra in the visible region [32–35]. Thus, we choose 7-diethylaminocoumarin as the fluorophore for fluorescence lifetime imaging. Pyridine group as acceptor for H^+, when N atom on pyridine group combines with H^+, it shows stronger electron absorption ability. Moreover, the photophysical properties of the probe are changed through the alteration in the electron absorption capacity. Therefore, we speculate that the fluorescence lifetime of the probe will change in acidic environment. The morpholine group can target the probe to the lysosomes, so that the change in the lysosomal acidity can be detected by fluorescence lifetime in Scheme 1. Based on the above reasons, we designed and synthesized the probe **PLN**, and detected the change of pH value in lysosome by FLIM. Detailed synthesis steps and characterization are shown in the Supporting information.

We firstly determined the absorption and emission spectra of **PLN** in Britton-Robison buffer solutions with various pH values. The absorption peak of **PLN** in different pH solutions only took little redshift in Fig. S6 (Supporting information). The excitation and emission spectrum of **PLN** in pH 7.04 solution was shown in Fig. S7 (Supporting information), the maximum excitation peak of **PLN** is 471 nm, the maximum emission peak is 596 nm, and the Stokes shift is about 120 nm. The fluorescence spectrum of **PLN** in varied pH solution was shown in Fig. 1A, and the maximum emission peak of **PLN** at 596 nm exhibits a large variation in fluorescence intensity. When the pH values in the solution gradually decreased from 10.12 to 2.04, the fluorescence intensity decreased by approximately 48 times. This may be because the N atoms on **PLN-H** pyridine combine with free hydrogen ions in the acidic environment to form N positive ions, which enhances the charge absorption, thereby enhancing the intramolecular charge transfer (ICT) effect of **PLN-H** and quenching the fluorescence. The fluorescence emission intensity of **PLN** has a good linear fit ($R^2 = 0.9956$) to the pH value of the solvents (the curve in Fig. 1A). The calculated p*K*a value is 3.88, indicating that **PLN** is suitable for monitoring the pH fluctuations of lysosomes with weak acidity (Fig. S8 in

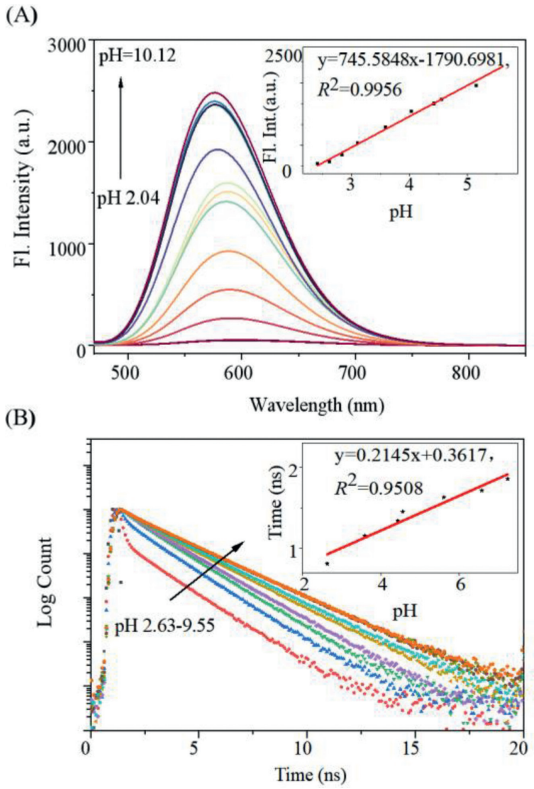

Fig. 1. (A) Fluorescence emission spectra of **PLN** (10 μmol/L) in BR buffer at different pH values (λex = 460 nm); (B) Fluorescence decays of **PLN** in BR buffer at different pH values (2.63–9.55), λex = 500 nm, λem = 550–800 nm.

Supporting information). In addition, the interference tests showed that the active substance had no effect on the emission intensity of **PLN** in the solutions of pH 3.11 and 9.06 in Fig. S9 (Supporting information). In order to verify the suitability of **PLN** in fluorescence lifetime imaging, we determined the fluorescence lifetime of **PLN** in Britton-Robison (BR) buffer solutions with different pH values (Fig. 1B). As we expected, the fluorescence lifetime of **PLN** increases regularly with the increase of pH value. The fluorescence lifetime of **PLN** is linearly fit ($R^2 = 0.9508$) to the pH values of the solvent with a fine linearity (the curve in Fig. 1B). The result shows that the lower the pH value, the shorter the fluorescence lifetime. As shown in Figs. S10A and B (Supporting information), solvent polarity and viscosity have almost no influence on the detection of **PLN**. Photophysical experimental results proved that the intrinsic fluorescence lifetime of the probe **PLN** could be used to determine pH changes in biological environment by FLIM technology. Before performing intracellular experiments, a standard MTT assay was performed to assess the cytotoxic effect of **PLN**. **PLN** was found to exhibit negligible cytotoxicity, as nearly 95% of 4T1 cells remained visible even though the concentration of **PLN** reaches 50 μmol/L (Fig. S11 in Supporting information). The results proved that the probe **PLN** had a good bio-compatibility and was competent to be a useful tool to detect the pH in biological systems. Consequently, to investigate the subcellular localization properties of **PLN**, the commercially available lysosomal specific dye, Lyso Tracker Blue, was co-incubated with **PLN** in normal 4T1 cells (Fig. S12 in Supporting information). Granular dots were observed in both red and blue channels, which are typical shapes of lysosomes. Pearson's co-localization coefficient was as high as 0.88. The overlapping curve of the two channels further confirmed **PLN** has a fine lysosomal labeling ability. Experimental results show that in living cells, **PLN** has an excellent ability to target lysosomes.

Encouraged by the above experimental results, we applied the probe **PLN** to cellular fluorescence lifetime imaging. First, we detected the pH difference of lysosomes in different cell lines by using **PLN**. In this work, 3T3, 4T1 and PC12 cell lines were incubated with **PLN** and used for fluorescence lifetime imaging. As shown in Fig. S13 (Supporting information), the difference in average lifetime of **PLN** in 3T3, 4T1 and PC12 were slightly. The fluorescence lifetime decay curves of **PLN** in a, b and c are illustrated in Fig. S14 (Supporting information). More interestingly, we could observe pH differences in individual lysosomes due to the quantitative characteristics of the fluorescence lifetime and the sensitivity to the pH of **PLN**. Thus, the magnified diagrams of the four pH gradients lysosomes at a, b, c in Fig. S13 are used to analyze the different pH individual lysosomes with the fluorescence lifetime of **PLN**. In 3T3 cells, the fluorescence lifetime of **PLN** at the four gradients in lysosomes of region of interest (ROI) a1–ROI a4 is 2.055 ± 0.012 ns to 2.433 ± 0.024 ns. Histograms of fluorescence lifetime values correspond to Fig. S13B. The fluorescence lifetime fitting curve of **PLN** in ROI a1–ROI a4 is illustrated in Fig. S15A (Supporting information). While in 4T1 and PC12 cells, the fluorescence lifetime at the four gradients in lysosomes of ROI b1-ROI b4 (1.981 ± 0.013 ns to 2.312 ± 0.027 ns) and ROI c1–ROI c4 (1.865 ± 0.015 ns to 2.201 ± 0.018 ns) was lower than that of 3T3 cells in general. The fluorescence lifetime in numerical histogram is correspondent to Figs. S13C and D, respectively. The fluorescence lifetime decay curves of **PLN** in ROI b1–ROI b4 and ROI c1–ROI c4 are illustrated in Figs. S15B and C (Supporting information). This may be because 3T3 is normal cell lines, while 4T1 and PC12 are cancer cell lines. As we known, the lysosomal pH of normal cells is slightly higher than that of cancer cells [40,41]. In conclusion, this result indicated that the acidity of a single lysosome can be quantified by the variations in the fluorescence lifetime of **PLN**, and normal cells and cancer cells can be differentiated by the acidity of lysosomes.

In order to detect the pH difference exhibited by lysosomes in different extracellular pH environments, we cultured 4T1 cells under different pH environments, thus changed the pH of lysosomes by adjusting the pH environment inside the cells. As illustrated in Fig. S16 (Supporting information), as cells are cultured in BR buffer of pH 5.15, the cells shrink into clusters immediately, and the targeted organelles of **PLN** are in vague in the meantime. The average lifetime of **PLN** in cells in acidic environment is estimated to be 2.064 ± 0.014 ns. Interestingly, while the pH value comes to 5.93, the probe targeted lysosomes significantly. Then, the average fluorescence lifetime of **PLN** increases to 2.366 ± 0.006 ns. When the pH value increases up to 8.08, the cells become slightly swollen in alkaline. Simultaneously, the average lifetime of **PLN** was 2.300 ± 0.009 ns, which was almost unchanged compared with the average fluorescence lifetime at pH value of 7.01. The fluorescence lifetime decay curves of **PLN** in these four pH environment stimulated cells are illustrated in Fig. S17 (Supporting information). This result indicated that the average lifetime of **PLN** gradually increased in cells with the increasing pH values in the environment, and the *pseudo*-color gradually changed from blue (shorter lifetime) to green (longer lifetime).

In addition, various drugs have a great influence on the acidity of lysosomes in cells, and the acidity of lysosomes will affect the physiological metabolism of cells. Therefore, visualization of lysosomal acidity is very critical to clarify the process of drug induced cell metabolism. Respectively, carbamazepine, ATP, chloroquine and NH_4Cl were cultured in 4T1 cells to establish cell pathological models of different lysosomal acidity in this study. Among them, ATP and carbamazepine drugs can reduce the pH value of lysosomes [1,39]. Nevertheless, chloroquine and NH_4Cl can reduce the concentration of proton in lysosomes and induce the increase of pH value in lysosomes [21,36–38]. As depicted in Fig. 2A in cabamzepine and ATP-stimulated cells, the fluorescence lifetime *pseudo*-color of **PLN** is almost blue, and that of control group is cyan. While in chloroquine and NH_4Cl-stimulated cells, *pseudo*-color of **PLN** is yellow. As the pH in lysosomes increases, the fluorescence lifetime of **PLN** gradually increases. The fluorescence lifetime decay curves of **PLN** in a, b, c, d and e of Fig. 2A are illustrated in Fig. S18 (Supporting information) when ATP and carbamazepine stimulated cells, the average fluorescence lifetime of **PLN** were 2.245 ± 0.017 ns and 2.277 ± 0.007 ns. The average fluorescence lifetime of **PLN** in cells of control group is estimated to be 2.339 ± 0.014 ns. The *pseudo* color changed from blue to green. However, to the chloroquine and NH_4Cl stimulated cells, the fluorescence lifetime increased up to 2.424 ± 0.010 and 2.424 ± 0.013 ns, and the *pseudo*-color changed from green to yellow. The results confirmed that the fluorescence lifetime of **PLN** had accurate response to variations in lysosomal acidity. Besides, to examine the pH difference of individual lysosomes in different drug-stimulated cells, four acidity gradients of lysosomes at a, b, c, d and e in Fig. 2 are individually enlarged partially. The fluorescence lifetime *pseudo*-color of **PLN** gradually changes from blue to green in lysosomes with four acidity gradients. The large fluorescence lifetime difference in numerical histogram is correspondent to Figs. 2B and C, and the fluorescence lifetime decay curves of **PLN** in ROI a1–ROI a4 and ROI b1–ROI b4 are illustrated in Figs. S19A and B in Supporting information. In the cells stimulated by carbamazepine and ATP, the fluorescence lifetime of **PLN** in the four acid gradients of lysosomes are determined from 1.890 ± 0.010 ns to 2.192 ± 0.014 ns (ROI a1–ROI a4) and from 1.780 ± 0.017 ns to 2.178 ± 0.013 ns (ROI b1–ROI b4). In the control group, the fluorescence lifetime in numerical histogram was corresponded to Fig. 2D and the fluorescence lifetime decay curves of **PLN** in ROI c1–ROI c4 are illustrated in Fig. S19C (Supporting information). The fluorescence lifetime of **PLN** at the four gradients of lysosomes, ROI c1–ROI c4, was depicted from 1.941 ± 0.016 ns to 2.336 ± 0.012 ns.

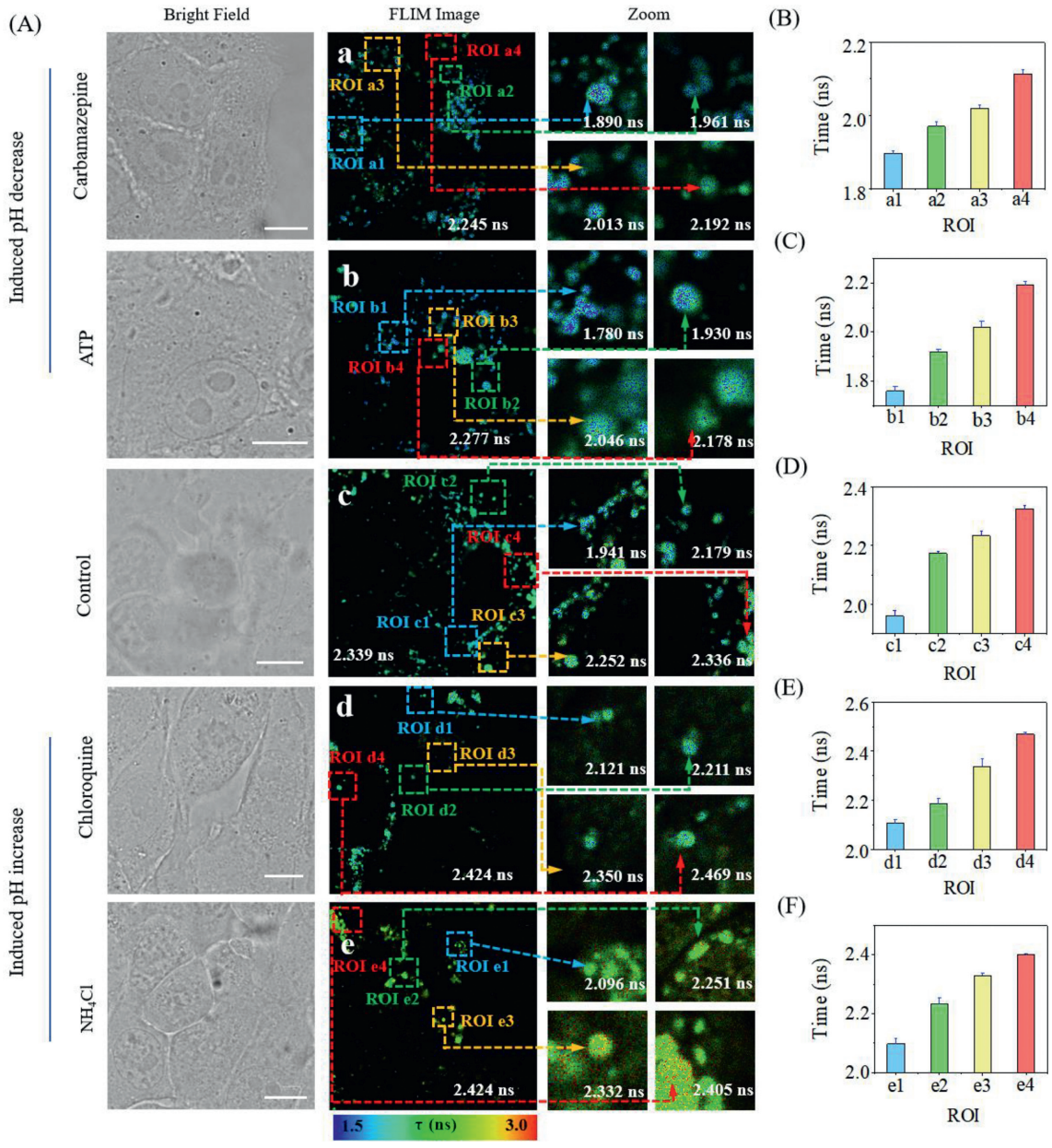

Fig. 2. (A) FLIM images of **PLN** (8 μmol/L) in control and cells stimulated by ATP, carbamazepine, chloroquine and NH_4Cl. (B) Histograms of the **PLN** fluorescence lifetime in ROI a1–ROI a5. (C) Histograms of the **PLN** fluorescence lifetime in ROI b1–ROI b5. (D) Histograms of the **PLN** fluorescence lifetime in ROI c1–ROI c5. (E) Histograms of the **PLN** fluorescence lifetime in ROI d1–ROI d5. (F) Histograms of the **PLN** fluorescence lifetime in ROI e1–ROI e5. λex = 500 nm, λem = 550–800 nm. Scale bar: 10 μm.

To the cells stimulated by chloroquine and NH_4Cl, the fluorescence lifetime *pseudo*-color of **PLN** gradually changes from green to yellow in lysosomes with four acidity gradients. The large fluorescence lifetime difference in numerical histogram is correspondent to Figs. 2E and F, and the fluorescence lifetime decay curves of **PLN** in ROI d1–ROI d4 and ROI e1–ROI e4 are illustrated in Figs. S19D and E (Supporting information). The fluorescence lifetime of **PLN** at the four gradients in chloroquine and NH_4Cl of lysosomes is generally higher than that in the control group. The **PLN** has a large difference in fluorescence lifetime in lysosomes with four acidity gradients, ranging from 2.121 ± 0.009 ns to 2.469 ± 0.010 ns (ROI d1–ROI d2) and 2.096 ± 0.011 ns to 2.405 ± 0.014 ns (ROI e1–ROI e2), respectively. In conclusion, these experiments demonstrate that the acidity of individual lysosomes in cells can be quantified by the change in **PLN** fluorescence lifetime.

Based on the excellent characteristics of **PLN** for the quantitative detection of single lysosomes, we applied **PLN** to the detected the pH of different layers of tumor tissue. In this work, we injected 4T1 cells into subcutaneous tissues of nude mice to establish tumor models. All mice were purchased from School of Pharmaceutical Sciences, Guangxi Medical University, and the studies were approved by the Animal Ethical Experimentation Committee of Guangxi Medical University. All animals were kept during experiment according to the requirements of the National Act on the use of experimental animals (China). After 10 days, when the tumor grew to 1.2 cm, the tumor tissue was dissected for fluorescence lifetime imaging [42]. We then cut samples from the center of the tumor (ROI 1) at 0.6 cm from tumor boundary "a" in Fig. 3, the position (ROI 2) between the tumor center and edge at 0.3 cm from tumor boundary "b" in Fig. 3, and the tumor boundary position (ROI 3). After incubation of these samples with **PLN**, fluorescence lifetime imaging was performed. As depicted in Fig. 3A, the fluorescence lifetime of ROI 1, ROI 2 and ROI 3 are 2.228 ± 0.003 ns, 2.353 ± 0.006 ns, and 2.446 ± 0.008 ns, respectively. The *pseudo*-

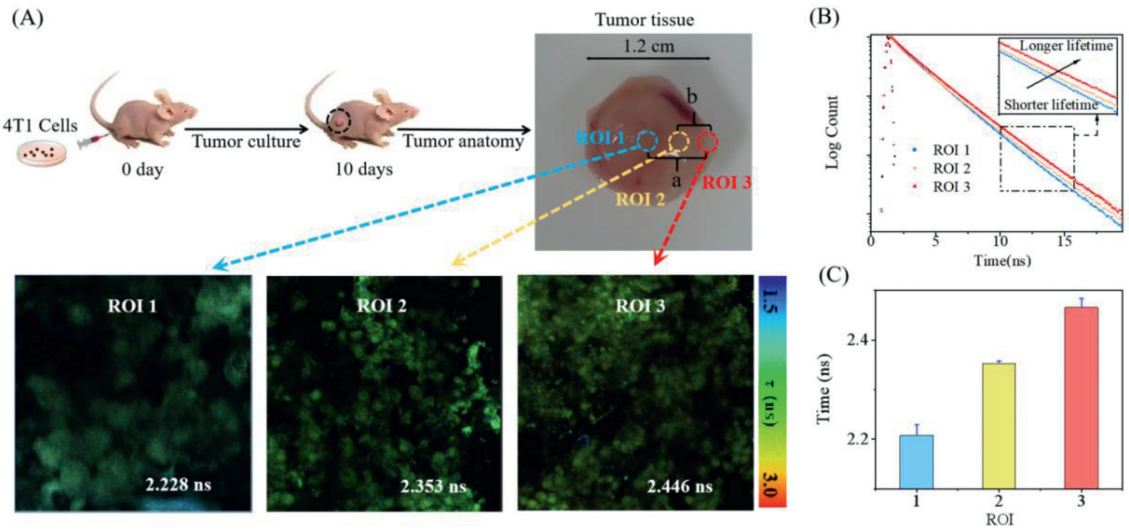

Fig. 3. (A) FLIM images and fluorescence decay of tumor stratification, "a" refers to the distance from ROI 1 to ROI 3, "b" refers to the distance from ROI 2 to ROI 3. (B) The fluorescence lifetime decay curve of **PLN** in ROI 1–ROI 3. (C) Histograms of the **PLN** fluorescence lifetime in ROI 1–ROI 3. λex = 500 nm, λem = 550–800 nm.

color of fluorescent life gradually varies from cyan to green. The fluorescence lifetime decay curves of **PLN** in ROI 1–ROI 3 are illustrated in Fig. 3B, and the fluorescence lifetime difference in numerical histogram is correspondent to Fig. 3C. Compared with outer sections, the fluorescence lifetime of **PLN** in ROI 1 decreased obviously, which indicates that the micro-environmental acidity of tumor inner part improved accordingly. It maybe because the highly hard lump of the inner core shows that the accumulation of high-density cancer cells leads to the higher degree of hypoxia areas than that of outer slices [5]. Thus, this result suggests that the probe **PLN** can evaluate the acidic environment at different tumor stratification through FLIM imaging, which is of great significance in evaluating the effect of intervention or drug delivery after the clinical treatment of tumors.

In conclusion, we rationally constructed a novel pH-sensitive fluorescent probe **PLN**, which can monitor changes in lysosomal pH value. The probe **PLN** possesses advantages of sensitive response to pH changes, good selectivity and fine linear correlation between pH value and fluorescence lifetime. Co-localization experiments exhibited that **PLN** could track lysosomes. Most importantly, **PLN** can be used to quantify the pH of an individual lysosome *via* the change of fluorescence lifetime. The lower the lysosomal pH, the smaller the fluorescence lifetime of **PLN**. In different external pH environments of cells, and under the stimulation of different drugs, the pH difference of intercellular lysosomes can be detected by **PLN** through FLIM imaging. Most of all, **PLN** is activated in the tumor micro-acid environment to trigger its layered determination of tumors at different levels. As the tumor depth increased, the fluorescence lifetime of **PLN** gradually decreased, indicating that the pH value inside the tumor gradually decreased, which may be due to the pH value of the high hardness lumps at the core of tumor was lower than that in the outer surface. Thus, the probe **PLN** can be used to evaluate the acidic environment at tumors stratification by FLIM imaging, which underscores the great potential for highly effective tumor visualization, accurate tumor resection and more epidemiological studies on lysosomal pH value.

Declaration of competing interest

The authors declare that they have no known competing financial interests or personal relationships that could have appeared to influence the work reported in this paper.

Acknowledgments

This work was financially supported by the National Natural Science Foundation of China (Nos. 21877048, 22077048 and 22277014), Guangxi Natural Science Foundation (Nos. 2021GXNSFDA075003, AD21220061), and the Startup Fund of Guangxi University (No. A3040051003).

Supplementary materials

Supplementary material associated with this article can be found, in the online version, at doi:10.1016/j.cclet.2023.108408.

References

[1] C. Jedeszko, B.F. Sloane, Biol. Chem. 385 (2004) 1017–1027.
[2] A. Jemal, R. Siegel, J. Xu, CA Cancer J. Clin. 60 (2010) 277–300.
[3] A. Jemal, F. Brey, M.M. Center, et al., CA Cancer J. Clin. 61 (2011) 69–90.
[4] K. Hardonnière, L. Huc, O. Sergent, J.A. Holme, D. Lagadic-Gossmann, Semin. Cancer Biol. 43 (2017) 49–65.
[5] O. Trédan, C.M. Galmarini, K. Patel, I.F. Tannock, J. Natl. Cancer Inst. 99 (2007) 1441–1454.
[6] R.A. Gottlieb, A. Dosanjh, Proc. Natl. Acad. Sci. U. S. A. 93 (1996) 3587–3591.
[7] F. Galindo, M.I. Burguete, L. Vigara, et al., Angew. Chem. Int. Ed. 44 (2005) 6504–6508.
[8] L.L. Wu, X.L. Li, C.S. Huang, N.Q. Jia, Anal. Chem. 88 (2016) 8332–8338.
[9] W.W. Zhu, X.Y. Chai, B.G. Wang, et al., Chem. Commun. 51 (2015) 9608–9611.
[10] W.F. Niu, M. Nan, L. Fan, et al., Dyes Pigm. 126 (2016) 224–231.
[11] T. Myochin, K. Kiyose, K. Hanaoka, et al., J. Am. Chem. Soc. 133 (2011) 3401–3409.
[12] B.L. Dong, X.Z. Song, X.Q. Kong, et al., J. Mater. Chem. B 5 (2017) 988–995.
[13] T.A. Davies, R.E. Fine, R.J. Johnson, et al., Biochem. Biophys. Res. Commun. 194 (1993) 537–543.
[14] F.Q. Yu, X.Y. Jing, W.Y. Lin, Anal. Chem. 91 (2019) 15213–15219.
[15] Y.X. Shi, X.C. Meng, H.R. Yang, J. Mater. Chem. B 7 (2019) 3569–3575.
[16] P. Wang, J.X. Huang, Y.Q. Gu, RSC Adv. 6 (2016) 95708–95714.
[17] T. Dhawa, A. Hazra, A. Barma, RSC Adv. 10 (2020) 1550–15513.
[18] M.L. Pei, X. Jia, G.P. Li, P. Liu, Mol. Pharm. 16 (2019) 227–237.
[19] Q.B. Zeng, Q.N. Guo, Y.P. Yuan, et al., ACS Appl. Biol. Mater. 3 (2020) 1779–1786.
[20] K. Yu, Y. Ding, H. Yu, et al., ACS Sens. 7 (2022) 1867–1873.
[21] Z.Y. Li, X.L. Cui, M.M. Xiao, et al., Dyes Pigm. 193 (2021) 109481.
[22] Y. Urano, D. Asanuma, Y. Hama, et al., Nat. Med. 15 (2009) 104–109.
[23] Y. Yan, X. Zhang, X. Zhang, et al., Chin. Chem. Lett. 31 (2020) 1091–1094.
[24] L. Gui, K. Wang, Y. Wang, et al., Chin. Chem. Lett. 34 (2023) 107586.
[25] H. Wang, Y. Sun, X. Lin, et al., Chin. Chem. Lett. 34 (2023) 107626.
[26] P. Guan, S. Shi, T. Zhang, et al., Dyes Pigm. 205 (2022) 110545.
[27] M.Y. Chin, A.R. Patwardhan, K.H. Ang, et al., ACS Sens. 6 (2021) 2168–2180.
[28] S. Burgstaller, H. Bischof, T. Gensch, et al., ACS Sens. 4 (2019) 883–891.
[29] R.B. Thompson, J.R. Lakowicz, Anal. Chem. 65 (1993) 853–856.
[30] J.R. Lakowicz, H. Szmacinski, Sens. Actuators B: Chem. 11 (1993) 133–143.
[31] H. Szmacinski, J.R. Lakowicz, Anal. Chem. 65 (1993) 1668–1674.

[32] J. Ma, W. Li, J. Li, et al., Talanta 182 (2018) 464–469.
[33] J. Yang, X. Liu, Z. Liu, et al., J. Mater. Chem. C 8 (2020) 2442–2450.
[34] X. Chen, Q. Chen, M. Chen, et al., Sens. Actuators B: Chem. 329 (2021) 129104.
[35] Y. Zhang, H. Teng, Y. Gao, et al., Chin. Chem. Lett. 31 (2020) 2917–2920.
[36] C.W. Chang, W.H. Tsai, W.J. Chuang, et al., J. Biomed. Sci. 14 (2007) 419–427.
[37] G. Niu, P. Zhang, W. Liu, et al., Anal. Chem. 89 (2017) 1922–1929.
[38] L.B. Shih, H.H. Lu, H. Xuan, D.M. Goldenberg, Int. J. Cancer 56 (1994) 538–545.
[39] X.J. Liu, X.Y. Liang, J. Guo, Insect Mol. Biol. 31 (2022) 60–72.
[40] S.Y. Kim, A. Podder, H. Lee, et al., Chem. Sci. 11 (2020) 9875–9883.
[41] Y. Song, H.X. Zhang, X. Wang, et al., Anal. Chem. 93 (2021) 1786–1791.
[42] X. Song, R. Wang, J. Gao, et al., Chin. Chem. Lett. 33 (2022) 1567–1571.